Optical measurements for determination of distances and deformations

Tiago Fernando Ribeiro Fernandes Araújo Gouveia, Military Academy / IST

***Abstract*—With the technological advances and the ambition of exploring new scientific areas, a quick evolution of metrology was verified. This evolution was important in the creation and development of new technological concepts. Optical metrology had a fast development with the creation of laser sources, enhancing important technological advances like significant increases in the quality of distance measurements, vibrations or deformations in equipment or structures.**

In this paper, it will be presented the triangulation method applied to distance measurement, as well as one of the techniques that work based on it - shadow Moiré. For this technique, this paper will refer its applications, advantages and disadvantages. The theoretical concepts behind it will also be presented and explained.

For the shadow Moiré technique several experiments were assembled, with the main purpose of validating the distance measurement device that was created – this device is referred through this dissertation as profilometer. Another objective is to study the results obtained by different configurations of the shadow Moiré technique and to compare them with the results obtained by the classic configuration.

***Index Terms*—Triangulation, Shadow Moiré, Profilometer**

I. Introduction

The development of a profilometer for surface digitalization using non-invasive measurement techniques is utterly important, since it is possible to advance in areas such as virtual reality or reverse engineering [1]. These techniques consist mainly on the emission of a signal – radio, sonic or ultrasonic – over a surface, recovering the reflected signal and analyzing it to retrieve the corresponding distance [1].

The possible applications of the device extend from industrial control, where it can be used to measure the deformation level of certain components, for the characterization and digitalization of surface profiles for quality control and for robotics, where it can be used for obstacle detection systems of remote controlled vehicles and smart robots [2].

On the military domain, this industrial control can be used in the manufacture of military material, which needs to fulfill additional requirements related to safety and robustness and has a stricter control applied to it. Another possible application on this matter is to be applied on the security and surveillance of military facilities.

There are several methods to perform non-invasive distance measurement. Among them, the method of triangulation was used to perform the described experiments. There has been a significant progress of optical measurement systems through recent years, mainly because of the increased understanding of basic physical principles and theoretical information about the detection range [1].

II. Triangulation

The triangulation method applied to distance measurement has its oldest references to the Greek philosopher and mathematician Thales of Miletus, who around 600 B.C[1] used this method to determine the height of the Giza pyramids and to determine the distance to a ship that was in the sea [3].

An example of the principle used in this method is represented in Figure 1:

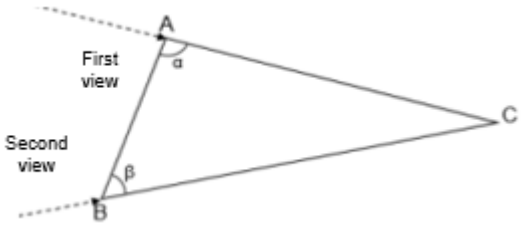

Figure 1 – Method of Triangulation [4]

Knowing the distance between A and B and the values of angles α and β, it is possible to use trigonometric relations to determine the distances between A and C and between B and C, who have currently an unknown value. The trigonometric relation between these points and angles are described by Expression (1):

$$\frac{\sin\alpha}{BC} = \frac{\sin\beta}{AC} = \frac{\sin(\pi-\alpha-\beta)}{AB} \quad (1)$$

Through Expression (1), it is possible to determine the expressions for distances *AC* and *BC*, given in Expressions (2) and (3), respectively [5]:

$$AC = \frac{AB\sin\beta}{\sin(\alpha+\beta)} \quad (2)$$

$$BC = \frac{AB\sin\alpha}{\sin(\alpha+\beta)} \quad (3)$$

Given these expressions, all of the distances of the triangle *ABC* can be determined, including the pretended distance *AC*.

There are three optical measurement techniques who use the triangulation method as its basic principle: laser scanning, Shadow Moiré and fringe projection. Each one of these techniques has its own advantages, disadvantages and principles of distance measurement. Nonetheless, the technique used during the experiments was the Shadow Moiré technique, since it has a simple configuration, is fast and is cheaper to perform than other techniques. Moreover, the identified disadvantages of this technique didn't apply in a laboratorial environment. This fact along with the identified advantages of the technique made it the chosen one to use in the proposed experiments.

The Shadow Moiré technique will be described in detail on the next chapter.

III. SHADOW MOIRÉ TECHNIQUE

The Shadow Moiré technique has its principles based on the triangulation method, as exposed above. The word "moiré" has its origins in the French literature and is often used to name a silk fabric which is composed by two layers. The movement of these layers creates some patterns on the fabric which are very similar to waves and named Moiré fringes or Moiré patterns [6]

The functioning principle of the technique is this: a grating composed by alternating opaque and transparent stripes with the same width is placed in front of the target object or surface. Posteriorly, a light source illuminates the surface from a certain direction, which projects a shadow of the grating fringes over the surface [7]. This shadow will be observed from another direction, and from the optical interference caused by the projected shadow and the observed image on the camera direction will result the so-called Moiré fringes [7]. The scheme for this technique can be seen in Figure 2, represented below:

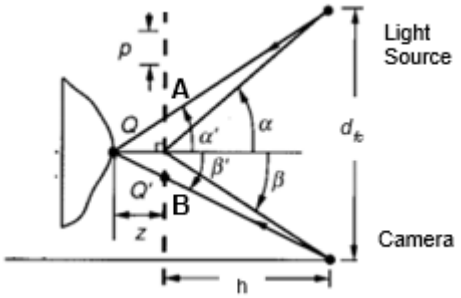

Figure 2 – Representation of Shadow Moiré technique [7]

Analyzing the Figure 2, the implementation of this technique can be well understood. Since the values of distances h and d_{fc} are fixed and known, as well as the period p that represents the distance between two fringes of the same opacity, the determination of the distance z between the grating and a point Q of the surface occurs in a simple manner [8]. The value of z is given at any point of the surface by Expression (4) [8]:

$$z = \frac{N \times p}{\tan\alpha' + \tan\beta'} = \frac{\Phi.p.l}{2\pi w} \qquad (4)$$

In Expression (4), N is the number of fringes which are situated between A and B, and the angles α' and β' are the illumination and visualization angles on the object surface, respectively. These angles are different from the angles α and β, who represent the illumination and visualization angles on the grating surface, respectively [8].

Generally, there is a phase shifting technique associated with moiré techniques. This phase shifting technique consists in the variation of the distance between the grating and the light source. Since this distance varies, the phase of the light beam will also vary, according to the expressions that define propagation of a light beam in space. For each distance variation, an image must be captured in order to capture the corresponding phase shift. From the application of this technique results a better and more precise phase map, since most of the resulting ambiguities and errors are corrected when compared to a phase map obtained with only one image.

After obtaining the images with the phase shifts, it is necessary to obtain the absolute phase map that, for each pixel, will retrieve the correspondent distance, according to Expression (4). However, the phase determination involves a series of steps, which will now be presented. First, it is necessary to consider a sensitivity calibration algorithm, which will retrieve the sensitivity as a statistical parameter for validation of the experiment results. This algorithm was proposed by *Du, Wang, Zhao* and *Jia* and is described in the reference [9].

After the application of the sensitivity calibration algorithm, it is necessary to transform the pixel intensities in the corresponding phases. The PCA algorithm is responsible for this part of the process, and it is described in the reference [10].

However, the phase values retrieved by the PCA algorithm are wrapped in the interval]-π,π], as it can be seen in reference [10]. Therefore, the obtained phase map is not absolute, since there will be multiple distance values corresponding to the same phase values, which invalidates the use of Expression (4) [11]. Due to this question, it is necessary to retrieve the absolute phase map with the absolute phase values for each pixel. This way the phase map can be represented correctly, and the Expression (4) can now be applied. The operation that retrieves the absolute phase map from the wrapped phase map is called "phase unwrapping". The algorithm used for phase unwrapping was the Goldstein algorithm, and it is described on references [12] and [13].

Once the absolute phase map is obtained, the distance map can now be determined. The transformation of the phase map into distance is done according to the sensitivity calibration algorithm described on reference [9].

IV. SHADOW MOIRÉ EXPERIMENT

In order to validate the proper use of the Shadow Moiré technique, an experiment was conducted. For the computerized component of the experiment, some scripts were created in the software Matlab 2014b.

Note that the script used for the PCA algorithm was obtained in [10]. The script used for the Goldstein algorithm was obtained through reference [14].

The experiment was conducted as represented in Figure 3:

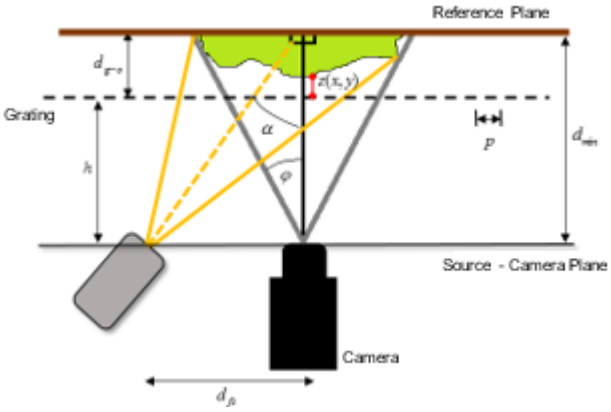

Figure 3 – Experiment schematic representation

The material used in the experiment was the following: (1) camera Canon 700D [15] (2) headphones JBL T450BT (3) 1 mm period grating (4) *Newport M-460-X Series* grating support (5) *Epson EB-S03* LCD light projector [16]. The experiment was assembled as represented in Figure 4:

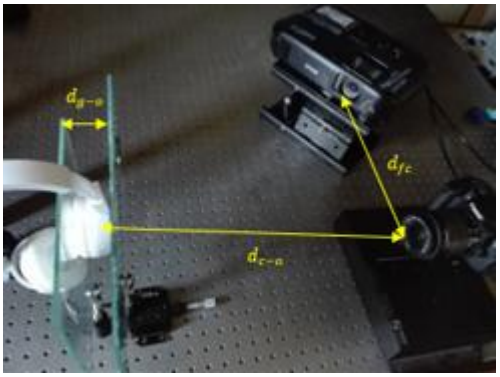

Figure 4 – Assembled Shadow Moiré experiment

The distances used in the experiment were the following: camera-object distance (d_{c-o}) of 55 cm, source-camera distance (d_{fc}) of 55 cm and grating-object distance (d_{g-o}) of 3 cm.

During the experiment, a set of 11 images were obtained. Each one of these images were captured with a uniform shift of Δh=0.5 mm compared to the previous image. This set is represented in Figure 5:

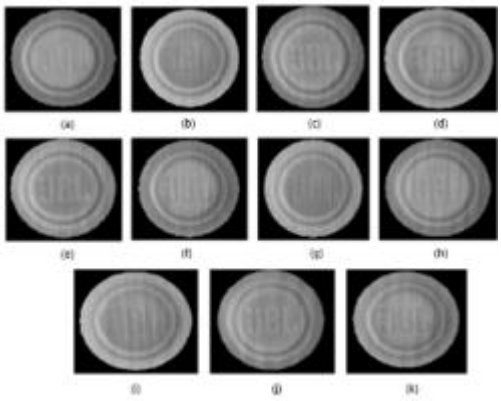

Figure 5 – Image set of Shadow Moiré experiment

Posteriorly, some image processing techniques were applied to the set of Figure 5. These techniques combined contrast enhancement techniques and noise suppression techniques through image filtering with an area of 30x30 pixels. After the application of these image processing techniques, a new set of images was obtained. After obtaining this new set, the algorithm expressed in [9] was followed. Considering it, the set of Figure 5 was divided in two different subsets: the first subset contained the images from (a) to (j); the second subset contained the images from (b) to (k). From these subsets resulted the corresponding non-absolute phase maps after the application of PCA algorithm, represented in Figure 6:

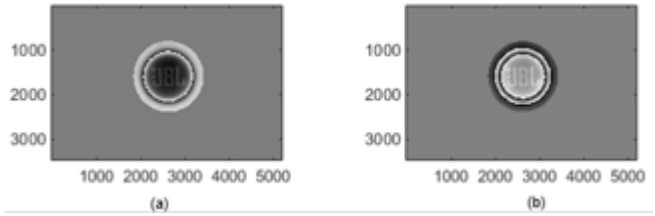

Figure 6 – Non-absolute phase maps obtained from Figure 5: (a) first subset; (b) second subset;

After the application of Goldstein algorithm to the previous phase maps, the absolute tridimensional phase map was obtained, which is represented in Figure 7:

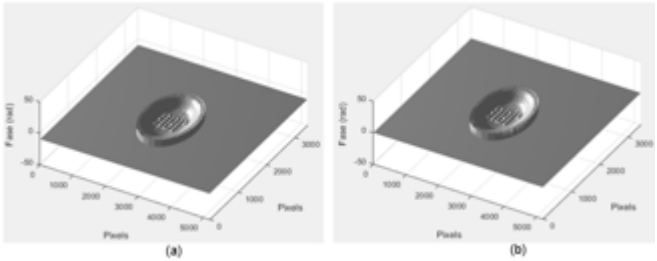

Figure 7 – Tridimensional absolute phase maps obtained with Goldstein algorithm: (a) first subset; (b) second subset;

Considering the sensitivity calibration algorithm expressed in [9], the distance map was obtained. This map is represented in Figure 8:

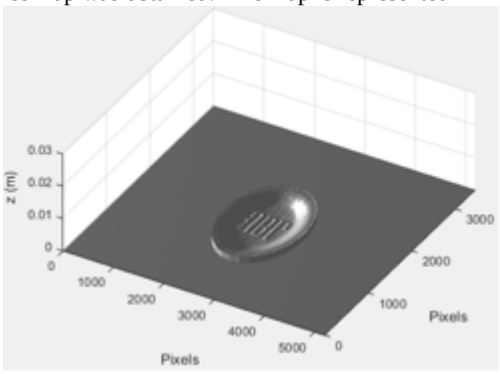

Figure 8 – Distance map obtained from the absolute phase maps

From the analysis of Figure 8, the results obtained show the reliability of the experiment. The distance difference between the highest and lowest plane is of 1.75 mm. This value is concordant with the measured value before the experiment, which was of 2±0.5 mm. Furthermore, the visual shape of the object that was obtained is identical to the original shape of the tested object.

To validate mathematically the obtained results, some statistical parameters were determined – sensitivity, standard deviation and standard error. For the sensitivity, the sensitivity calibration algorithm described in [9] was again considered. Using the phase maps of Figure 7, the obtained sensitivity map is represented in Figure 9:

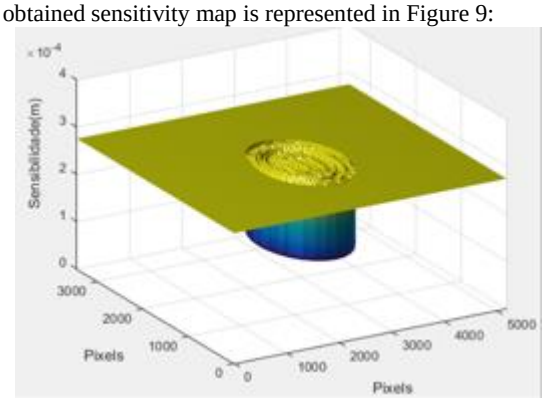

Figure 9 – Obtained sensitivity of measurement

The sensitivity results exposed in Figure 9 show that these are uniform for the entire image. This feature is important, since it influences the obtained distance map in a direct manner. Additionally, it can also be noted that the obtained sensitivity has values of 0.28 mm. This result validates the experiment for the measurement of small distances, since it shows that is capable of detecting very small changes in the surface topography.

Posteriorly, the values of standard deviation and standard error were determined. To obtain them, five sets of images identical to the set of

Figure 5 were captured. Then, the standard deviation was determined for each pixel, and is shown in Figure 10:

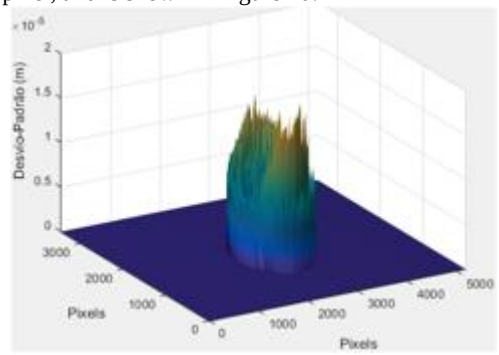

Figure 10 – Standard deviation obtained from the experiment

The maximum standard deviation obtained is from 0.015 mm, to which corresponds a maximum standard error of 0.0067 mm. Therefore, the obtained results in the experiment were determined with a precision of 0.0067 mm in the worst case. This precision value validates these results, since it confirms the possibility of measuring very small distances and obtaining an identical surface compared with the original surface.

V. Additional Experiments with Shadow Moiré

After validation of the previous results, obtained with the Shadow Moiré technique, other variations of this technique were tested. Those variations occurred not only in the physical configurations of the Shadow Moiré technique, but also at the several stages of the distance measurement process – like the image processing stage. The main objective of this variations was to understand the influence that each of the components of the experiment has in the obtained results.

A. Shadow Moiré with two projectors

This variation of the classic technique consists on the use of two projectors illuminating the target surface instead of one as in the classic technique. The objective is to understand the effects of light intensity on the results. The experiment was assembled following the scheme represented in Figure 11.

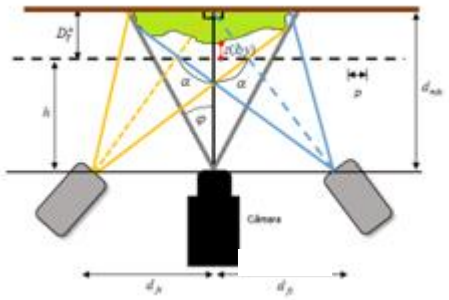

Picture 11 – Scheme representation of Shadow Moiré technique with two projectors

Since the objective is to evaluate the effect of light intensity, all the other parameters have to remain the same. Therefore, the materials and values of the distances and angles remain the same as the ones stated in Chapter IV.

The experiment was assembled as represented in Figure 12:

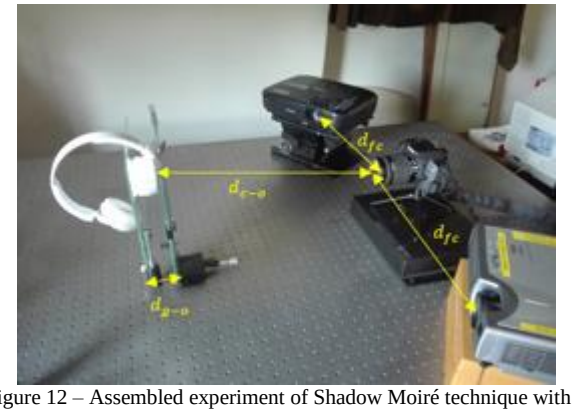

Figure 12 – Assembled experiment of Shadow Moiré technique with two projectors

During the experiment, a set of 11 images were obtained. Each one of these images were captured with a uniform shift of $\Delta h = 0.5$ mm compared to the previous image. This set is represented in Figure 13:

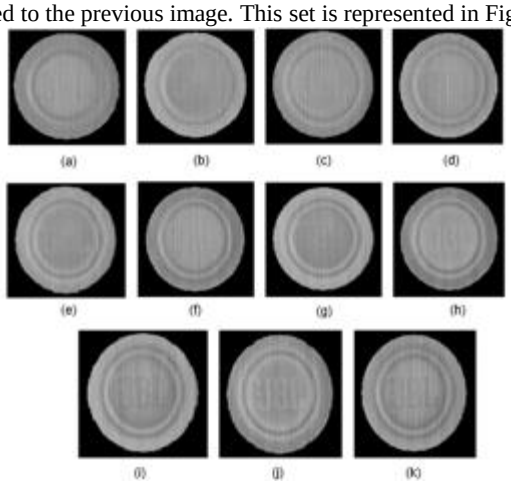

Figure 13 – Image set of Shadow Moiré experiment with two projectors

After this set was obtained, another set resulted from image processing techniques, which were the same as the ones applied in Chapter IV. After obtaining this new set of images, the algorithm expressed in [9] was followed. Considering it, the set of Figure 13 was divided in two different subsets: the first subset contained the images from (a) to (j); the second subset contained the images from (b) to (k). From these subsets resulted the corresponding non-absolute phase maps after the application of PCA algorithm, represented in Figure 14:

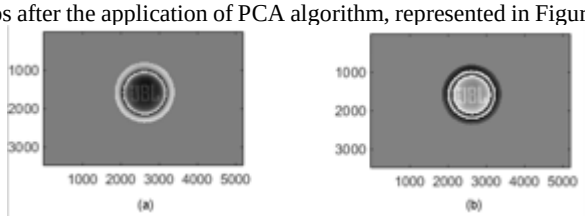

Figure 14 – Non-absolute phase maps obtained from Figure 13: (a) first subset; (b) second subset;

After the application of Goldstein algorithm to the previous phase maps, the absolute tridimensional phase map was obtained, and is represented in Figure 15:

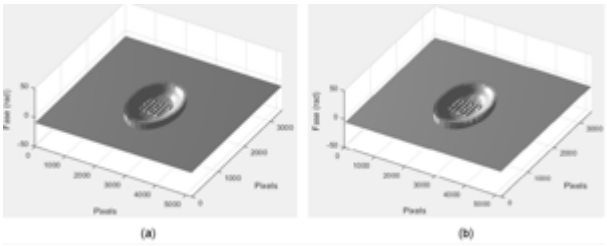

Figure 15 – Tridimensional absolute phase maps obtained with Goldstein algorithm: (a) first subset; (b) second subset;

Considering the sensitivity calibration algorithm expressed in [9], the distance map was obtained. This map is represented in Figure 16:

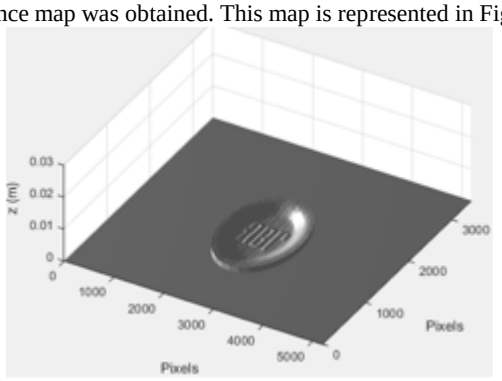

Figure 16 – Distance map obtained from the absolute phase maps (larger scale)

The results obtained by this variation of the classic technique were very similar to the ones obtained by its classic counterpart.

The resulting error from this technique compared to the classic version is exposed in Figure 17:

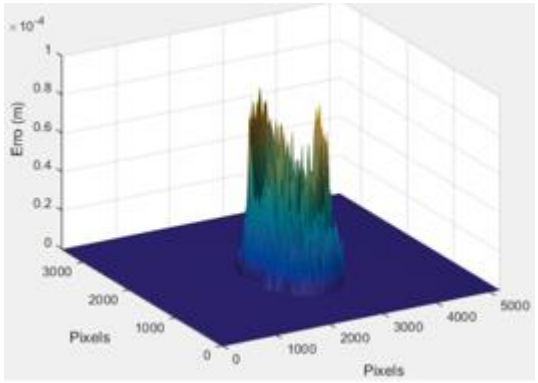

Figure 17 – Error between the results obtained with classic Shadow Moiré and its two projectors variant

From the analysis of Figure 17, it is visible that the maximum error obtained between the two variations of the Shadow Moiré technique is of 0.085 mm. Therefore, it can be concluded that the Shadow Moiré technique with two projectors is also a valid technique for distance measurement.

B. Shadow Moiré with Double Parallel Grating

This variation of the classic technique consists on the use of two gratings with parallel fringes between them. The objective is to understand the effect created by the interaction between the two gratings on the object, and the correspondent phase shift. Another objective was to check if a reliable distance map could be obtained without noise interference. The experiment was assembled following the scheme represented in Figure 18.

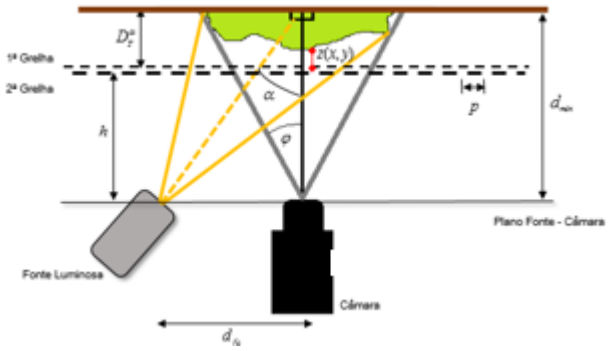

Figure 18 – Scheme representation of Shadow Moiré technique with two projectors

Since the objective is to evaluate the effect of the double grating, all the other parameters have to remain the same. Therefore, the materials and values of the distances and angles remain the same as the ones stated in Chapter IV. Also, since the experiment consists on the placement of two parallel gratings between the same glasses, the assemble is the same as seen in Figure 4.

During the experiment, a set of 11 images were obtained. Each one of these images were captured with a uniform shift of Δh=0.5 mm compared to the previous image. This set is represented in Figure 19:

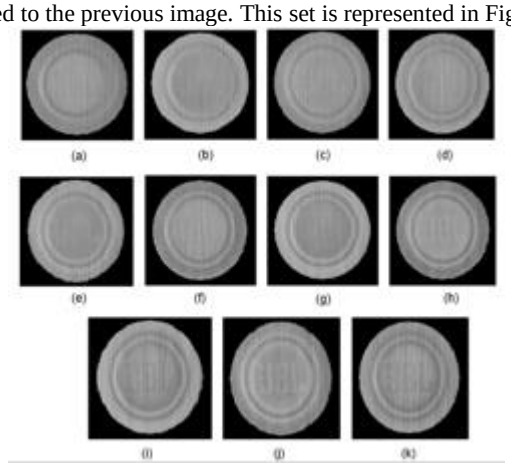

Figure 19 – Image set of Shadow Moiré experiment with double parallel grating

After this set was obtained, another set resulted from image processing techniques, which were the same as the ones applied in Chapter IV. After obtaining this new set of images, the algorithm expressed in [9] was again followed. Considering it, the set of Figure 19 was divided in two different subsets: the first subset contained the images from (a) to (j); the second subset contained the images from (b) to (k). From these subsets resulted the corresponding non-absolute phase maps after the application of PCA algorithm, represented in Figure 20:

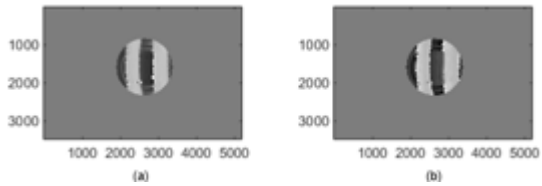

Figure 20 – Non-absolute phase maps obtained from Figure 19: (a) first subset; (b) second subset;

After the application of Goldstein algorithm to the previous phase maps, the absolute tridimensional phase map was obtained, and is

represented in Figure 21:

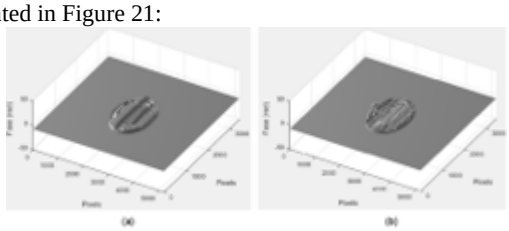

Figure 21 – Tridimensional absolute phase maps obtained with Goldstein algorithm: (a) first subset; (b) second subset;

Considering the sensitivity calibration algorithm expressed in [9], the distance map was obtained. This map is represented in Figure 22:

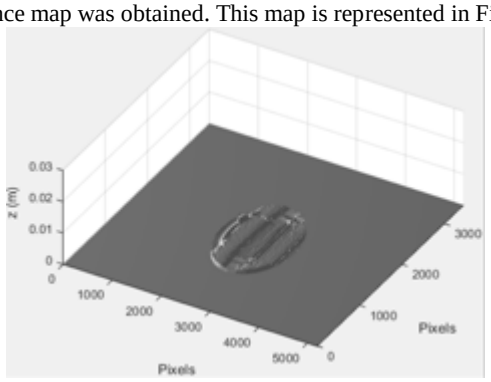

Figure 22 – Distance map obtained from the absolute phase maps

The results obtained by this variation of the classic technique were very different to the ones obtained by its classic counterpart. This is due to the noise caused by the double grid, whose interference caused

The resulting error from this technique compared to the classic version is exposed in Figure 23:

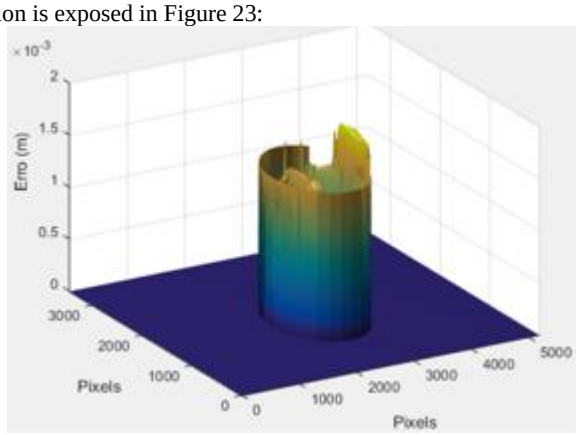

Figure 23 – Error between the results obtained with classic Shadow Moiré and its double parallel grating variation

From the analysis of Figure 23, it is visible that the maximum error obtained between the two variations of the Shadow Moiré technique is of 1.5 mm. This result is very inaccurate, since it is very different from the original shape of the object. Therefore, it can be concluded that the Shadow Moiré technique with double parallel grating is not a valid technique for distance measurement.

C. Shadow Moiré with Double Perpendicular Grating

This variation of the classic technique consists on the use of two gratings with the fringes placed perpendicularly between gratings. Due to the similarities with the experiment conducted in subchapter B, the physical parameters and assembly of the present experiment are identical to that experiment. Therefore, the scheme of the experiment is represented in Figure 18 as well.

Since the objective is to evaluate the effect of light intensity, all the other parameters have to remain the same. Therefore, the materials and values of the distances and angles remain the same as the ones stated in Chapter IV. Also, since the experiment consists on the placement of two perpendicular gratings between the same glasses, the assemble is the same as seen in Figure 4.

During the experiment, a set of 11 images were obtained. Each one of these images were captured with a uniform shift of Δh=0.5 mm compared to the previous image. This set is represented in Figure 24:

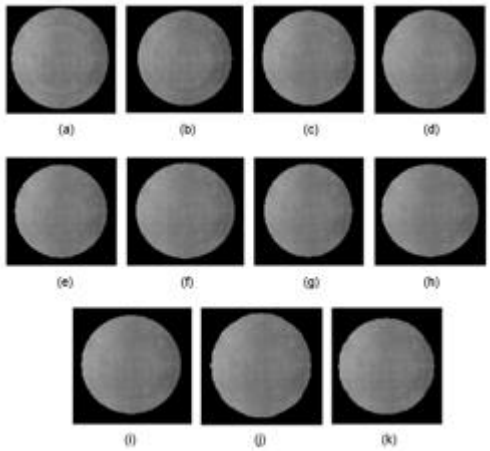

Figure 24 – Image set of Shadow Moiré experiment with double perpendicular grating

After this set was obtained, another set resulted from image processing techniques, which were the same as the ones applied in Chapter IV. After obtaining this new set of images, the algorithm expressed in [9] was again followed. Considering it, the set of Figure 24 was divided in two different subsets: the first subset contained the images from (a) to (j); the second subset contained the images from (b) to (k). From these subsets resulted the corresponding non-absolute phase maps after the application of PCA algorithm, represented in Figure 25:

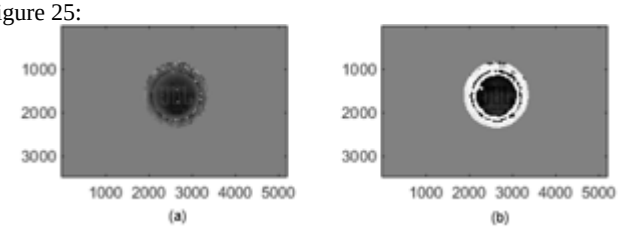

Figure 25 – Non-absolute phase maps obtained from Figure 24: (a) first subset; (b) second subset;

After the application of Goldstein algorithm to the previous phase maps, the absolute tridimensional phase map was obtained, and is represented in Figure 26:

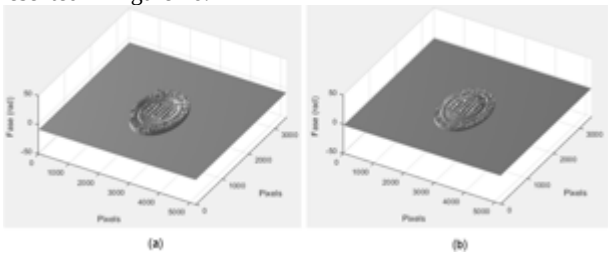

Figure 26 – Tridimensional absolute phase maps obtained with Goldstein algorithm: (a) first subset; (b) second subset;

Considering the sensitivity calibration algorithm expressed in [9], the distance map was obtained. This map is represented in Figure 27:

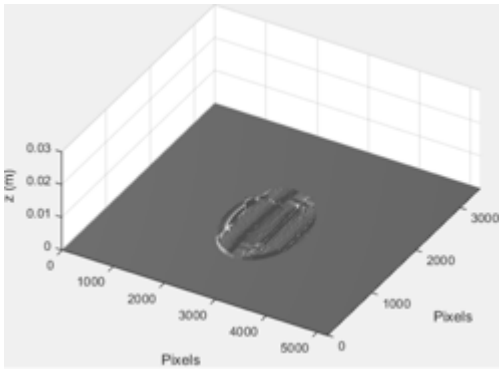

Figure 27 – Distance map obtained from the absolute phase maps

The resulting error from this technique compared to the classic version is exposed in Figure 28:

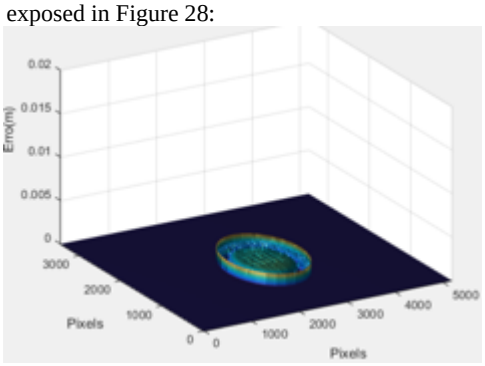

Figure 28 – Error between the results obtained with classic Shadow Moiré and its double parallel grating variation

From the analysis of Figure 28, it is visible that the maximum error obtained between the two variations of the Shadow Moiré technique is of 1.5 mm. Although the result obtained by this variation allows to see some features of the object, the result is not accurate when comparing with the classic version of Shadow Moiré technique. Therefore, it can be concluded that the Shadow Moiré technique with double perpendicular grating is not a valid technique for distance measurement.

D. Shadow Moiré with Double Parallel Separated Grating

This variation of the classic technique consists on the use of two gratings with parallel fringes between them. However, in this variation the two gratings are not in the same plane. Instead, one of the gratings will be moved with a constant step *Δh'*, while the other will remain in a fixed position (*h*). The objective is to understand the effect created by the interaction between the two gratings on the object, and the correspondent phase shift. Another objective was to check if a reliable distance map could be obtained without noise interference. The experiment was assembled following the scheme represented in Figure 29.

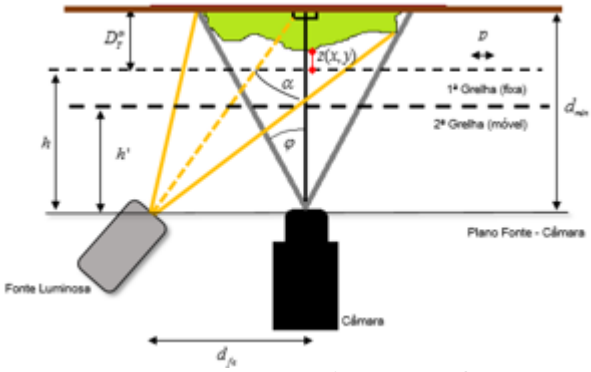

Figure 29 – Scheme representation of Shadow Moiré technique with two projectors

Since the objective is to evaluate the effect of the double grating on the results, all the other parameters have to remain the same. Therefore, the materials and values of the distances and angles remain the same as the ones stated in Chapter IV.

During the experiment, a set of 3 images were obtained. Each one of these images were captured with a uniform shift of Δh=2 mm compared to the previous image. This set is represented in Figure 30:

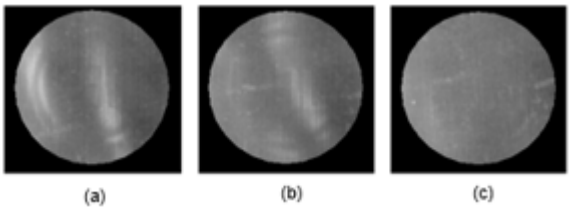

Figure 30 – Image set of Shadow Moiré experiment with double parallel grating

After this set was obtained, another set resulted from image processing techniques, which were the same as the ones applied in Chapter IV. After obtaining this new set of images, the algorithm expressed in [9] was again followed. Considering it, the set of Figure 30 was divided in two different subsets: the first subset contained the images (a) and (b); the second subset contained the images (b) and (c). From these subsets resulted the corresponding non-absolute phase maps after the application of PCA algorithm, represented in Figure 31:

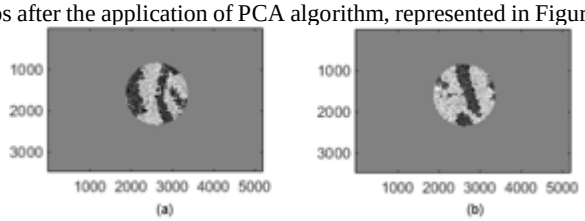

Figure 31 – Non-absolute phase maps obtained from Figure 30: (a) first subset; (b) second subset;

After the application of Goldstein algorithm to the previous phase maps, the absolute tridimensional phase map was obtained, and is represented in Figure 32:

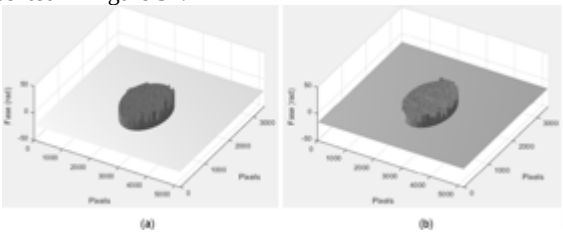

Figure 32 – Tridimensional absolute phase maps obtained with Goldstein algorithm: (a) first subset; (b) second subset;

Considering the sensitivity calibration algorithm expressed in [9], the distance map was obtained. This map is represented in Figure 33:

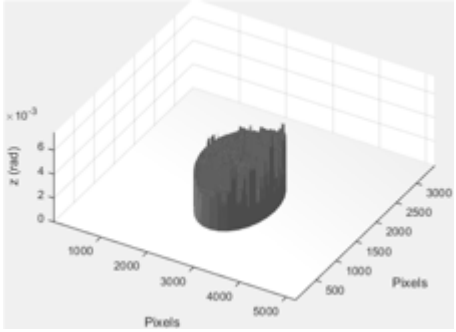

Figure 33 – Distance map obtained from the absolute phase maps

The resulting error from this technique compared to the classic version is exposed in Figure 34:

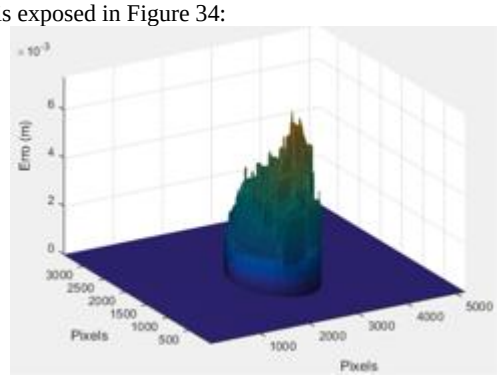

Figure 34 – Error between the results obtained with classic Shadow Moiré and its double parallel grating variation

From the analysis of Figure 34, it is visible that the maximum error obtained between the two variations of the Shadow Moiré technique is of 6 mm. This result is the most inaccurate so far, since it is very different from the original shape of the object. This is due to several factors: first, the double grating that introduces much noise and interference; second, the successive layers of glass contribute for the reduced visibility of the object; third, the reduced number of images from the set contributes for the bad quality of the distance map. Therefore, it can be concluded that the Shadow Moiré technique with double parallel separated grating is not a valid technique for distance measurement.

E. Shadow Moiré with Double Perpendicular Separated Grating

This variation of the classic technique consists on the use of two gratings with perpendicular fringes between them. However, in this variation the two gratings are not in the same plane. Instead, one of the gratings will be moved with a constant step *Δh'*, while the other will remain in a fixed position (*h*). This experiment is identical to the one described in subchapter D. The objective is to understand the effect created by the interaction between the two gratings on the object, and the correspondent phase shift. Another objective was to check if a reliable distance map could be obtained without noise interference. Since the scheme of this experiment is identical to the one described previously, the same is represented in Figure 29.

Since the objective is to evaluate the effect of the double grating on the results, all the other parameters have to remain the same. Therefore, the materials and values of the distances and angles remain the same as the ones stated in Chapter IV.

During the experiment, a set of 3 images were obtained. Each one of these images were captured with a uniform shift of Δh=2 mm compared to the previous image. This set is represented in Figure 35:

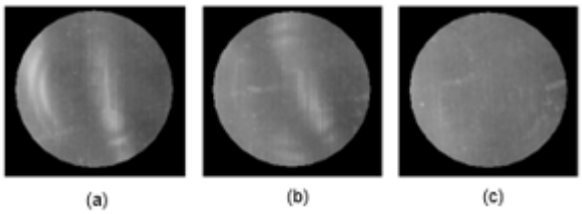

Figure 35 – Image set of Shadow Moiré experiment with double parallel grating

After this set was obtained, another set resulted from image processing techniques, which were the same as the ones applied in Chapter IV. After obtaining this new set of images, the algorithm expressed in [9] was again followed. Considering it, the set of Figure 35 was divided in two different subsets: the first subset contained the images (a) and (b); the second subset contained the images (b) and (c). From these subsets resulted the corresponding non-absolute phase maps after the application of PCA algorithm, represented in Figure 36:

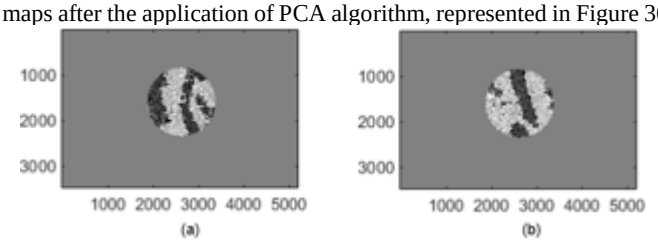

Figure 36 – Non-absolute phase maps obtained from Figure 35: (a) first subset; (b) second subset;

After the application of Goldstein algorithm to the previous phase maps, the absolute tridimensional phase map was obtained, and is represented in Figure 37:

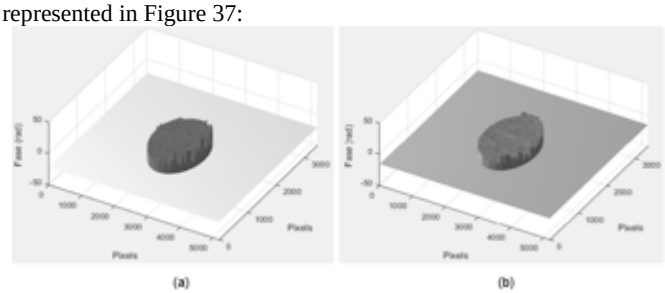

Figure 37 – Tridimensional absolute phase maps obtained with Goldstein algorithm: (a) first subset; (b) second subset;

Considering the sensitivity calibration algorithm expressed in [9], the distance map was obtained. This map is represented in Figure 38:

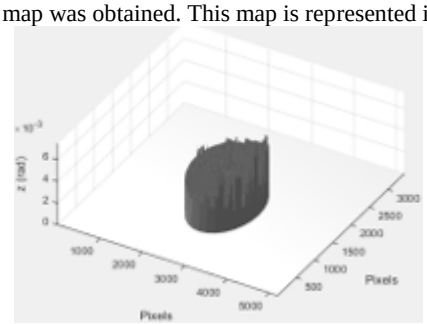

Figure 38 – Distance map obtained from the absolute phase maps

The resulting error from this technique compared to the classic version is exposed in Figure 39:

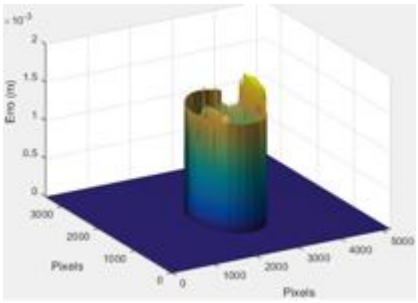

Figure 39 – Error between the results obtained with classic Shadow Moiré and its double parallel grating variation

From the analysis of Figure 39, it is visible that the maximum error obtained between the two variations of the Shadow Moiré technique is of 6 mm. This result is the most inaccurate so far, since it is very different from the original shape of the object. This is due to several factors: first, the double grating that introduces much noise and interference; second, the successive layers of glass contribute for the reduced visibility of the object; third, the reduced number of images from the set contributes for the bad quality of the distance map. Therefore, it can be concluded that the Shadow Moiré technique with double parallel separated grating is not a valid technique for distance measurement.

F. Effect of Image Processing Techniques on the Results

This experiment consists on changing the parameters used in image processing techniques that were applied to the image set. The objective is to observe and understand the effect that the image processing techniques have in the obtained results with Shadow Moiré technique. To evaluate this, two experiments were assembled, each one of them related to one of the image processing techniques used during the experiment of Chapter IV – contrast enhancement and noise filtering.

The results of the experiments are expressed throughout this subchapter.

To evaluate the effect caused by the contrast enhancement technique, the experiment assembled used the image set of Figure 5. From there, two different distance maps were obtained: to obtain the first map, the contrast enhancement technique was used, but the second map did not use this technique. Apart this single difference, all the remaining procedures used to obtain the distance map are identical to the ones used in Chapter IV. The results are expressed in Figure 40:

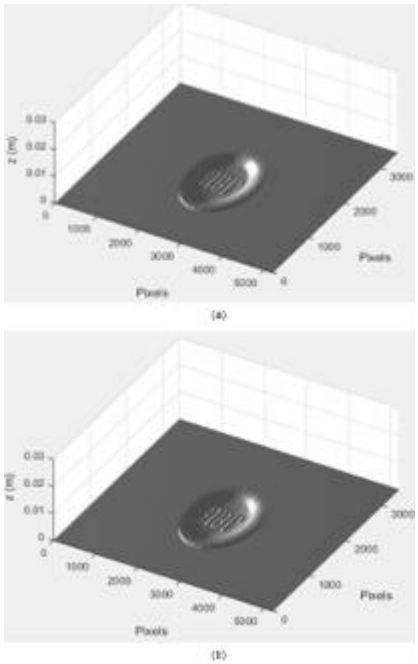

Figure 40 – Effect of contrast enhancement technique: (a) distance map with contrast enhancement; (b) distance map without contrast enhancement

Through Figure 40, it can be seen that the results obtained are not very different from each other in this case. However, it was observed that the contrast enhancement technique allowed the distance map to have a smaller difference between consecutive phase values, which results in a brighter and smoother profile distance map on the first case.

For the noise filtering technique, the assembled experiment obtained four different distance maps. Each of these maps used a different area for noise filtering: no filter, 30x30, 60x60 and 90x90 pixels. All the remaining processes were followed identically to Chapter IV. The results are expressed in Figures 41 and 42:

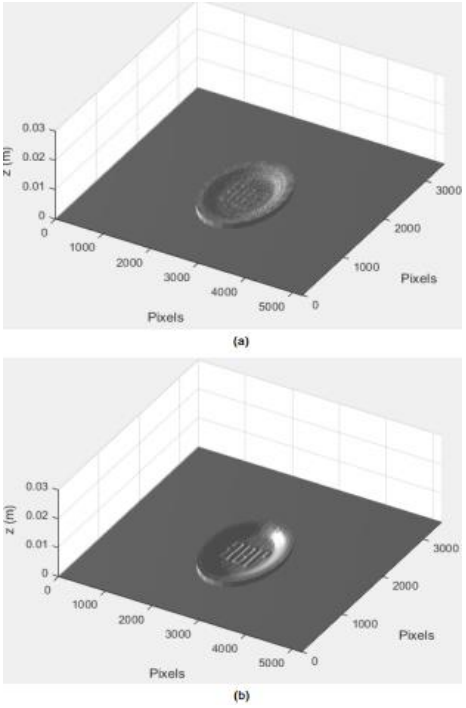

Figure 41 – Distance maps obtained with different filtering areas: (a) no filter; (b) 30x30 pixel filter

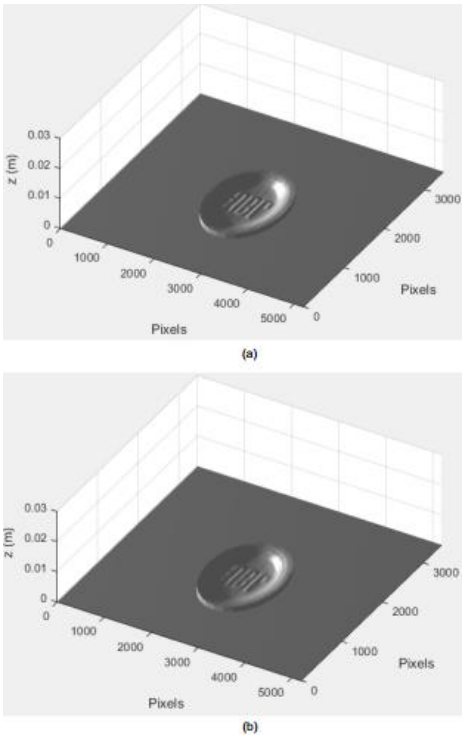

Figure 42 – Distance maps obtained with different filtering areas: (a) 60x60 pixel filter; (b) 90x90 pixel filter

Through Figures 41 and 42, it is possible to observe the effect of the filtering area in the results. As expected, the non-application of noise filtering techniques originates errors in the determination of the distance map. This effect is visible in Figure 41(a), where the noise existence prevented the correct determination of the distance map. Atop of this, the steps caused by the fringe interference are very clear in the obtained map of Figure 41(a). These steps are created by the difference between the pixels associated to the grating and the object. The progressive loss of spatial resolution is very clear with the increase of the filtering area. However, the decrease of fringe effect in the distance map is also visible. It is also comprehensible that, when the filtering area increases, the phase values tend to lose the differences between them. In an extreme situation, the phase values might even be identical throughout the whole image, thus the whole spatial resolution being lost. Therefore, the filtering area shall always be defined with a commitment between noise filtering and spatial resolution.

VI. Conclusions

The possible applications for optical measurement devices comprise several areas. From industrial control applications, where they can be used for detection of irregularities or deformations in parts, to military applications, where they can be used to control the remote vehicles used for vigilance and security of military units.

Throughout this paper the method of triangulation was described, as well as the distance measurement technique that works based on it - the Shadow Moiré technique.

The Shadow Moiré technique is known as a cheap technique, because it has a simple configuration. It is a fast measurement technique, but it needs a previous preparation of the experiment, since the grating must be placed first in front of the target.

To validate the proposed configuration, an experiment was assembled. The experiment employed the Shadow Moiré technique to measure a target object. The results show that the technique is precise and can determine the profile of objects correctly.

Furthermore, some experiments to evaluate the effects of the several components of Shadow Moiré technique were conducted. These experiments reveal that only one of the tested variations acquired results as precise as its classic counterpart.

In short, all the objectives were successfully completed.

References

[1] M.-C. Amann, T. Bosch, M. Lescure, R. Myllyla, and M. Rioux, “Laser ranging: a critical review of usual techniques for distance measurement,” *Opt. Eng.*, vol. 40, no. 1, pp. 10–19, 2001.

[2] F. Chen, G. Brown, and M. Song, “Overview of three-dimensional shape measurement using optical methods,” *Optical Eng.*, vol. 39, no. 1, pp. 10–22, 2000

[3] G. Berkovic & E. Shafir, “Optical methods for distance and displacement measurements,” *Advances in Optics and Photonics 4*, pp. 441-471, 11 Sep-2012.

[4] João Fonseca, Sistemas de medida de distância utilizando laseres e as suas aplicações, Masters Dissertation, Instituto Superior Técnico, 2016.

[5] R. Farcy, Applications des lasers - Principle optiques avec problèmes commentés, Paris: Masson, 1992.

[6] R.A.B. Jr, "Moiré Tutorial", [Online]. Disponível: http://www.deg.ufla.br/site/_adm/upload/file/Roberto/TutorialMOIRE.pdf. [Acedido em 04 Novembro 2016].

[7] A. J. Avilaq and A. H. Rezaie, “3D Face reconstruction using modified shadow moiré,” *2013 21st Iran. Conf. Electr. Eng. ICEE 2013*, pp. 3–7, 2013.

[8] K. Creath, J. Schmit, and J. C. Wyant, *Optical Metrology of Diffuse Surfaces*. 2006.

[9] H. Du, J. Wang, H. Zhao *et al*., “Calibration of the high sensitivity shadow moiré system using random phase-shifting technique”, *Optics and Lasers in Engineering*, vol. 63, pp. 70-75, 2014.

[10] J. Vargas, J. Quiroga e T.Belenguer, “Phase-shifting interferometry based on principal component analysis”, *Optics Letters*, vol. 36, no. 8, p. 1326, 2011.

[11] Gonçalo Matias, Radar Interferometry: 2D Phase Unwrapping via Graph Cuts, Masters Dissertation, Instituto Superior Técnico, 2006.

[12] R. Goldstein, H. Zebker, C. Werner, “Satellite radar interferometry: Two-dimensional phase unwrapping”, *Radio Science*, vol. 23, no. 4, pp. 713-720, 1988.

[13] D. Ghiglia, M. Pritt, Two-Dimensional Phase Unwrapping: Theory, Algorithms and Software, New York: Wiley, 1998.

[14] Bruce Spottiswoode, Javier Vargas, “Goldstein 2D Phase Unwrapping Algorithm”, [Online]. Available in http://www.mathworks.com/matlabcentral/fileexchange/22504 [Acessed in March 11, 2017].

[15] Epson, “EB-S03 LCD Light Projector” [Online]. Available in https://www.epson.pt/products/projectors/mobile/eb-s03#specifications [Acessed in September 09, 2017].

[16] Canon, “Canon EOS 700D – Technical Characteristics” [Online]. https://www.canon.pt/for_home/product_finder/cameras/digital_slr/eos_700d/specification.aspx [Acessed in September 09, 2017].